# Efficient multiple-reference-frame controller for current-harmonic suppression with a shunt active power filter

Miguel Ochoa Giménez, Javier Roldán Pérez, Aurelio García Cerrada, Juan Luis Zamora Macho
ICAI, Comillas Pontifical University, Madrid, Spain
E-mail: Miguel.Ochoa@iit.upcomillas.es

***Abstract*—This paper presents a control method based on multiple reference frames for tracking or rejecting periodic signals in the context of shunt active power filters in power systems. The proposed scheme allows recursive calculation when referring signals to reference frames rotating synchronously with harmonic space vectors; giving an accurate and efficient harmonic controller and avoiding most of the trigonometric functions. The description in this paper will focus on the controller basics, its implementation aspects and its performance. A scenario with grid-frequency variations will be considered to evaluate its adaptation capability.**

## I. Introduction

Steady-state voltages and currents in electric power systems consist of a fundamental component of 50 or 60Hz plus harmonics with frequencies which are integer multiples of the fundamental one. This description applies to balanced and unbalanced situations. Voltage and current harmonics are important concerns in electric power systems because they can be hazardous to elements connected to the grid [1] [2]. Harmonics are produced by non-linear devices such as AC-to-DC converters, arc furnaces, saturated transformers, etc. and have been traditionally tackled using LC-based passive filters which are simple, reliable and relatively lossless. Unfortunately, passive filters cannot be tuned during operation and can introduce unwanted resonances in power systems.

Nowadays, active power filters (APF) based on power electronics devices are a flexible alternative to compensate current and voltage disturbances [3]. An APF includes a power electronics converter that is controlled using closed-loop techniques to accurately suppress harmonic distortion. APF's can be implemented as shunt type (ShAPF), series type (SAPF), or a combination of these two types. Each topology is appropriate for a different set of load and/or supply line problems as shown in [4].

Proportional+Integral (PI) controllers using Park's Transformation of three-phase electrical variables into a synchronous reference frame is often used for power-flow control in power electronics devices. The speed of the synchronously-rotating frame is made equal to the positive sequence of the fundamental frequency so that all variables of that frequency are DC in steady state and simple PI controllers can be used [5]. However, harmonics are still seen as sinusoids in that frame and cannot be tackled so easily.

Harmonic control was first addressed using resonant terms as in ([6], [7] and [8]) and a more comprehensive approach was later found with the so-called "repetitive controller" which, basically, has a denominator such as $1-e^{-Ts}$ where $T$ is the period corresponding to the fundamental frequency of the grid magnitudes and $s$ is the Laplace variable. This controller has poles at $\pm h\omega_1 j$ with $h = 0, 1, 2\cdots$ being $\omega_1$ the fundamental frequency. In fact, the repetitive controller works as multiple selective controllers for all harmonics of interest. On one hand, this controller provides a very concise formulation, on the other hand, flexibility is lost when looking at individual harmonics. In addition, repetitive controllers are very sensitive to frequency variations and some approximation techniques have been reported to tackle this problem [9]).

The use of reference frames rotating synchronously with harmonic space vectors (harmonic synchronous reference frames or HSRFs) for active filters was proposed in [10]. In this approach, each harmonic is seen as a constant value after an appropriate Park's Transformation and PI controllers can be designed for each one, independently. This procedure has always been considered as cumbersome due to the calculation of many trigonometric functions in real-time. In the context of power active filters, [11] and [12] established the equivalence between controllers in a stationary reference frame (resonant controllers) and controllers in HSRF's (PI controllers). They suggest designing the controllers using HSRFs whilst implementing them as resonant controllers in a stationary reference frame to avoid computational burden.

Harmonic control can also e tackled using a DFT (Discrete Fourier Transform) or a DCT (Discrete Cosine Transform) as in [13], [14] and [15]. Both strategies have two main drawbacks: the sampling frequency has to be chosen carefully as a multiple of the fundamental frequency of the signals to be sampled and, secondly, storage of the DFT coefficients and management of the data buffers calculated for each harmonic brings a large computational effort, especially under grid frequency variations.

In this paper, the strategy based on HSRFs will be revisited showing that its implementation can be greatly eased whilst maintaining excellent performance. Besides, it will be demonstrated that designing and implementing the current regulators directly in each HSRF has many advantages. In the proposed controller, most trigonometric functions are

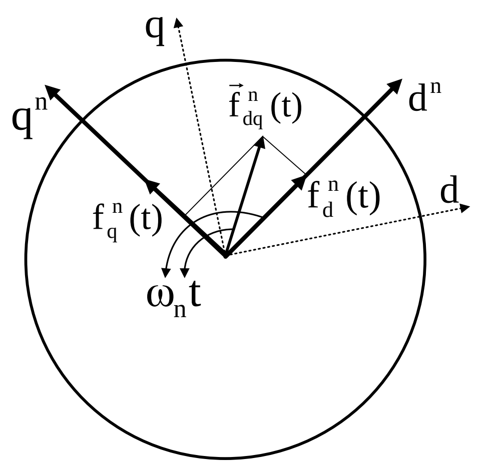


Fig. 1. Vector representation of a $dq$ signal in a harmonic synchronous reference frame $dq^n$

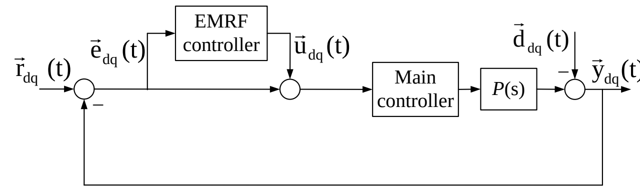


Fig. 2. Plug-in EMRF controller in relation to the main P-Q controller

avoided in order to reduce the computation effort. The variations in the grid frequency will be considered to show its frequency-adaptation capability.

## II. Efficient use of harmonic synchronous reference frames

When controlling voltage source converters (VSCs) connected to the grid in an ShAPF, natural magnitudes of the three-phase currents and voltages (*abc*) can be transformed into a vector signal (*dq0*) using Park's Transformation. For a generic three-phase variable:

$$\vec{f}_{dq0}(t) = \boldsymbol{P}(\theta)\vec{f}_{abc}(t) \tag{1}$$

where:

$$\boldsymbol{P}(\theta) = k_1 \begin{bmatrix} k_2 & k_2 & k_2 \\ cos(\theta) & cos(\theta - \frac{2\pi}{3}) & cos(\theta + \frac{2\pi}{3}) \\ -sin(\theta) & -sin(\theta - \frac{2\pi}{3}) & -sin(\theta + \frac{2\pi}{3}) \end{bmatrix} \tag{2}$$

Ideally, the vector $\vec{f}_{dq0}(t)$ will have constant *d-q* components in steady state if $\theta$ in (2) is chosen so that:

$$\theta = \theta_0 = \omega_0 t \tag{3}$$

where $\omega_0$ is equal to the frequency of the positive sequence of the fundamental harmonic of the grid variables. This property leads to the common representation of the positive sequence of electrical magnitudes as vectors which rotate with an angular speed $\omega_0$. A *d-q* axis coordinate system which rotates synchronously with these vectors can also be defined and all variables can be referred to this new system (see Fig. 1). It is then said that the electrical variables are referred to a synchronous *d-q* reference frame (SRF). If there are harmonics in the electrical variables, each one can be seen as a rotating space vector in the SRF used so far. Its angular speed will be (see Fig. 1):

$$\omega_n = \overbrace{(i \cdot m - 1)}^{n} \omega_0 \tag{4}$$

where $m$ is the harmonic order and $i = 1$ if the harmonic is of positive sequence and $i = -1$ if the harmonic is of negative sequence. The components $(d - q)$ of each harmonic will be DC magnitudes if the resulting rotating space vector is referred to a reference frame rotating with its angular speed (HSRF) which will be here named $dq^n$ reference frame. Accordingly, the measured signals have to be rotated many times, after using Park's Transformation, to extract harmonic information as DC magnitudes. Using a complex-number notation for any electric variable $v$, rotation is achieved as:

$$\begin{aligned} \vec{v}_{dq^n} &= v_{d^n} + jv_{q^n} = e^{-j\theta_n}\left(v_d + jv_q\right) & (5) \\ \theta_n &= \omega_n t & (6) \end{aligned}$$

where:

- $v_d$ and $v_q$ are the components of $\vec{v}$ in the SRF after Park's transformation.
- $e^{-j\theta_n}$ is a complex number with modulus equal 1 and phase equal $-\theta_n$
- $v_{d^n}$ and $v_{q^n}$ are the components of $\vec{v}$ in the $dq^n$ HSRF.

For example the 5th harmonic, which is typically of negative sequence, will be synchronous with a reference frame with $n = -6$ ($dq^{-6}$) whilst the 7th harmonic, which is typically of positive sequence, will be synchronous with a reference frame $n = 6$ ($dq^6$). In fact, all positive-sequence harmonics will have $n > 0$ and all negative-sequence harmonics will have $n < 0$.

The proposed controller is depicted in Fig. 2 and consists of (a) a "main controller" tailored to take care of the positive sequence of the fundamental component of the electrical variables (d-q), including active- and reactive-power-related issues; and (b) a "harmonic controller" placed as a "plug-in controller". Fig. 2 also includes the plant model $\boldsymbol{P}(s)$ and the relevant signals in the $dq$ reference frame such as the set point $\vec{r}_{dq}(t)$, the output variable $\vec{y}_{dq}(t)$, the control signal $\vec{u}_{dq}(t)$, the disturbance $\vec{d}_{dq}(t)$ and the error $\vec{e}_{dq}(t)$.

A PI controller for each harmonic, which is inside the "EMRF Controller" block depicted in Fig. 2, can be used to tackle the errors referred to each HSRF because each harmonic have now DC components at a given HSRF. The relative phase of each harmonic space vector in its reference frame is not required because the controller is designed to eliminate the direct and quadrature components of the harmonic errors.

The use of multiple rotations suggests that many $\cos(n\omega_o t)$ and $\sin(n\omega_o t)$ functions must be calculated and this would represent an unaffordable computational burden for most microprocessors. Fortunately, $\cos(n\omega_0 t)$ and $\sin(n\omega_0 t)$ can be easily calculated from $\cos(\omega_0 t)$ and $\sin(\omega_0 t)$, already calculated when performing Park's transformation in (1). In fact, using Moivre's formula [16]:

$$\overbrace{\cos(n\omega_0 t) + j\sin(n\omega_0 t)}^{\cos(\theta_n)+j\sin(\theta_n)} = [\cos(\omega_0 t) + j\sin(\omega_0 t)]^n \quad (7)$$

reducing the computational effort required for multiple-harmonic control as the trigonometric functions are transformed into sums and products. Furthermore, this calculation can be performed in a recursive way:

$$e^{j(n+1)\omega_o t} = [\cos(\omega_o t) + j\sin(\omega_o t)]^n\,[\cos(\omega_o t) + jsin(\omega_o t)] \quad (8)$$

where $\sin(\omega_o t)$ and $\cos(\omega_o t)$ are obtained for the main controller by means of a Phase-Locked Loop (PLL). At each HSRF, the DC-value components for each harmonic can be extracted using a low-pass filter and, therefore, a PI controller can be applied. The low-pass filter limits the speed of the transient response. Therefore, the bandwidth of this filter has to be chosen carefully (typically equal to 25 Hz).

The outputs of the HSRF controllers have to be rotated back into the fundamental $(d-q)$ reference frame where they can all be added together to produce the control signal. Each one of the rotations required uses the angle already calculated but in the opposite direction, and this operation does not require the evaluation of any trigonometric function either, because:

$$[\cos(\omega_o t) + j\sin(\omega_o t)]^{-n} = \cos(\omega_o t) - j\sin(\omega_o t) \quad (9)$$

resulting in the complex conjugate of (7).

So far, referring a space vector to a HSRF has been presented using complex-number notation but it can also be done using matrix notation with the following rotation matrix:

$$\boldsymbol{R}(n\omega_o t) = \begin{bmatrix} \cos(n\omega_o t) & -\sin(n\omega_o t) \\ \sin(n\omega_o t) & \cos(n\omega_o t) \end{bmatrix} \quad (10)$$

with:

$$\begin{bmatrix} v_d \\ v_q \end{bmatrix} = \boldsymbol{R}(n\omega_o t) \begin{bmatrix} v_{d^n} \\ v_{q^n} \end{bmatrix} \quad (11)$$

## III. Investigating the computational effort of the proposed approach

The harmonics typically present in a balanced three-phase system are $m = (6k\pm1)$ with $k = 1, 2, ..., 5$. If harmonics up to the 31st are considered, all HSRFs for $n = \pm 6k$ have to be calculated. To start with, $\sin(1\cdot\omega_0)$ and $\cos(1\cdot\omega_0)$ (HSRF with $n = 1$) are required but have already been calculated for the initial Park's transformation. The transformation into a HSRF with $n = 2$ can be done by using (8) whilst the combination of both HSRFs ($n = 1$ and $n = 2$) leads to the HSRF with $n = 3$. This process is repeated with $n = 3$ and $n = 3$ to obtain $n = 6$ and so on, until the HSRF with $n = 30$ is reached. All mathematical operations used are multiplications ($M$) and sums ($S$) and the total number of multiplications and sums performed, in this case, are:

- The computation of the reference frames rotating at $2\omega_0$, $3\omega_0$, $6\omega_0$, $12\omega_0$, $18\omega_0$, $24\omega_0$ and $30\omega_0$ implies: $7 \times (4M + 2S)$.
- The computation of the reference frames to refer the negative sequences require at $-2\omega_0$, $-3\omega_0$, $-6\omega_0$, $-12\omega_0$, $-18\omega_0$, $-24\omega_0$ and $-30\omega_0$ using (5) implies: $7 \times (1M)$.
- A first-order Butterworth filter at each harmonic of positive and negative sequence (both real and imaginary parts) implies: $5 \times 2 \times 2 \times (2M + 1S)$.
- The projection of error signal on the various reference frames ($n = \pm 6$, $n = \pm 12$, $n = \pm 18$, $n = \pm 24$, $n = \pm 30$) implies $10 \times (4M + 2S)$.
- The projection of the command signal on the dq ($n = 0$) frame $10 \times (4M + 2S)$.

Therefore, in this example, the back and forward transformation of signals bring 155 multiplications and 81 sums. Together with this computation load, the controller calculations and the initial Park's transformation must be taken into account.

## IV. Advantages of implementing HSRF's

Some advantages arise when HSRF's are implemented directly in a DSP. First, PI regulator can easily be designed. The situation of the efficient multiple-reference-frame controller (EMRF) is shown in Fig. 2. Other situations for the EMRF can be used. In order to design each of the PI controllers to be placed with in EMRF one should investigate the transfer-function matrix between $\vec{U}_{dq}$ and $\vec{E}_{dq}$ at each one of the frequencies (speeds of the synchronously-rotating frame) of interest, with the main-control loop closed. Therefore, one can define:

- $P'(s)_{dd}$ the transfer function $\frac{E_d(s)}{U_d(s)}$, $P'(s)_{qq}$ the transfer function $\frac{E_q(s)}{U_q(s)}$ and
- $P'(s)_{dq}$ the transfer function $\frac{E_d(s)}{U_q(s)}$, $P'(s)_{qd}$ the transfer function $\frac{E_q(s)}{U_d(s)}$

where $E_x(s)$ and $U_x(s)$ are the Laplace transform of $e_x$ and $u_x$, respectively ($x$ is $d$ or $q$). In addition, recalling that the use of the Park's transformation produces symmetric plants, one can write $P_p^{'}(s) = P'(s)_{dd} = P'(s)_{qq}$ and $P_c^{'}(s) = P'(s)_{dq} = P'(s)_{qd}$ and the errors produced in the SRF due to the input in the nth HSRF rotated to the SRF (with Laplace Transform $\vec{E}_{dq}(s)$) can be calculated as:

$$\begin{bmatrix} E_d(s) \\ E_q(s) \end{bmatrix} = -\begin{bmatrix} P_p^{'}(s) & -P_c^{'}(s) \\ P_c^{'}(s) & P_p^{'}(s) \end{bmatrix} \cdot \begin{bmatrix} U_d(s) \\ U_q(s) \end{bmatrix} \quad (12)$$

where $\vec{U}_{dq}(s)$ is the Laplace Transform of the input into the fundamental SRF. The relationship between $u_{dq}^n$ and $e_{dq}^n$ in

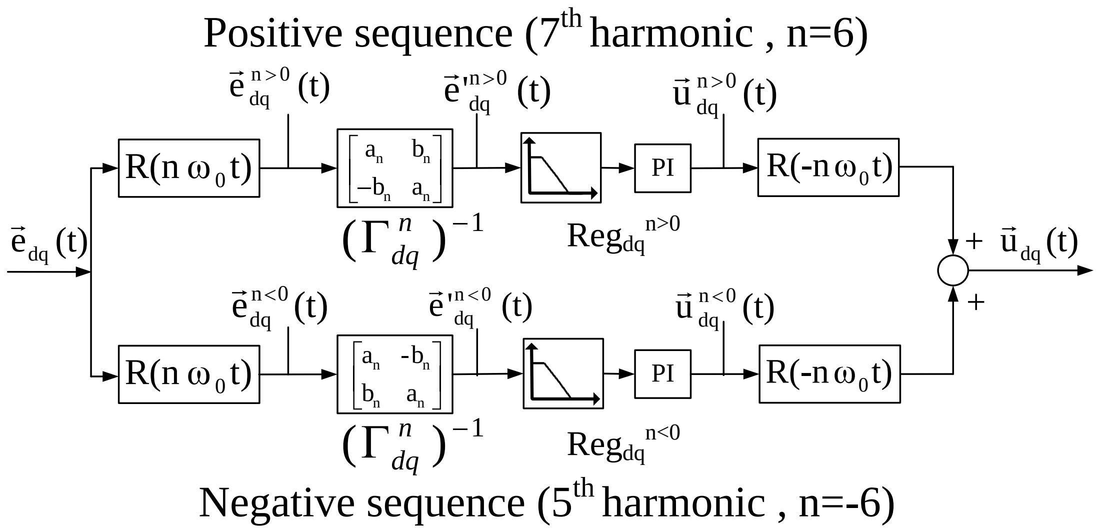


Fig. 3. Efficient-multiple-reference-frame controller scheme

the time domain can be obtained by calculating the inverse Laplace transform and rotating into each HSRF giving:

$$\begin{bmatrix} e_{d^n} \\ e_{q^n} \end{bmatrix} = -\underbrace{\begin{bmatrix} \{P_p^{'n}\}_a + \{P_c^{'n}\}_b & -(\{P_p^{'n}\}_b - \{P_c^{'n}\}_a) \\ \{P_p^{'n}\}_b - \{P_c^{'n}\}_a & \{P_p^{'n}\}_a + \{P_c^{'n}\}_b) \end{bmatrix}}_{\mathbf{\Gamma}_{dq}^n} \cdot \begin{bmatrix} u_{d^n} \\ u_{q^n} \end{bmatrix} \quad (13)$$

with

$$\{P_p^{'n}\}_a = |P_p^{'n}| \cos(\angle P_p^{'n}) \quad (14)$$
$$\{P_p^{'n}\}_b = |P_p^{'n}| \sin(\angle P_p^{'n}) \quad (15)$$
$$\{P_c^{'n}\}_a = |P_c^{'n}| \cos(\angle P_c^{'n}) \quad (16)$$
$$\{P_c^{'n}\}_b = |P_c^{'n}| \sin(\angle P_c^{'n}) \quad (17)$$

The inverse of $\Gamma_{dq}^n$ at each harmonic can be used to compensate the open-loop system and to decouple $\vec{u}_{dq^n}$ and $\vec{e}_{dq^n}$ using a new error signal $\vec{e}^{\,'}_{dq^n}$ written as:

$$\begin{bmatrix} e'_{d^n} \\ e'_{q^n} \end{bmatrix} = -\underbrace{(\mathbf{\Gamma}_{dq}^n)^{-1} \cdot \mathbf{\Gamma}_{dq}^n}_{\boldsymbol{I}} \cdot \begin{bmatrix} u_{d^n} \\ u_{q^n} \end{bmatrix} \quad (18)$$

where $\boldsymbol{I}$ is the identity matrix. A detailed view of the EMRF controller is depicted in Fig. 3, where $a_n$ is the element (1,1) of $(\mathbf{\Gamma}_{dq}^n)^{-1}$ and $b_n$ is the element (2,1) of $(\mathbf{\Gamma}_{dq}^n)^{-1}$.

Second, if $\mathbf{\Gamma}_{dq}^n$ is not exactly known, identification techniques have to be used at the start-up point and/or on-line. As all signal are DC magnitudes thanks to the HRSF's, the identification techniques are quite simple. Therefore, plant transfer functions are not necessary for the EMRF.

Finally, frequency adaptation capability is a clear advantage and it is a very useful feature because a small frequency variation in the fundamental component is amplified when considering higher-order harmonics. In the proposed EMRF, the fundamental frequency $\omega_0$ is measured and used in the HSRF's generation explicitly and, therefore, its adaptation is quite natural. Thanks to this feature, each harmonic regulator is tuned automatically at each sample period. The speed of this adaptation capability is only limited by the speed of the PLL.

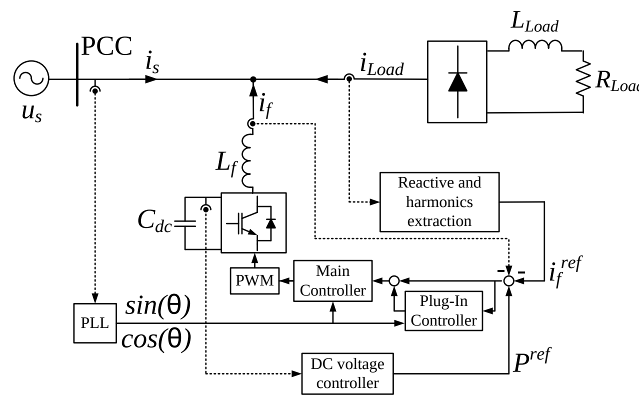


Fig. 4. Active power filter and control system scheme

## V. Simulation results

A shunt active power filter has been simulated using SIMULINK-SIMPOWER to illustrate the proposed control method. The nominal RMS voltage is 230 V and 50 Hz. The DC voltage of the VSC is 500 V. The VSC is connected to the grid using an inductance $L_f$ = 1.5 mH. The grid inductance is $L_s$ = 700 $\mu$H and the grid $X_s/R_s$ ratio is 10. A 5kVA rectifier-type of load is connected at the point of common coupling (PCC) to simulate the demand of harmonic currents. The inverter switching frequency was set at 5.4 kHz. The system set-up is depicted in Fig. 4: the EMRF controller is placed as a "plug-in" block on the top of a power flow controller (main controller); reactive power consumed by the load and the DC-voltage control of the

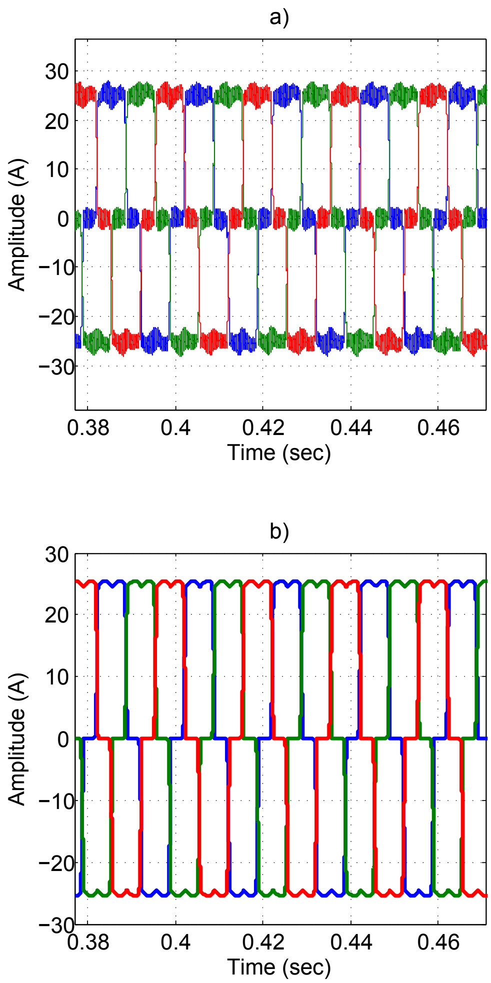


Fig. 5. Grid (a) and load (b) currents without ShAPF control.

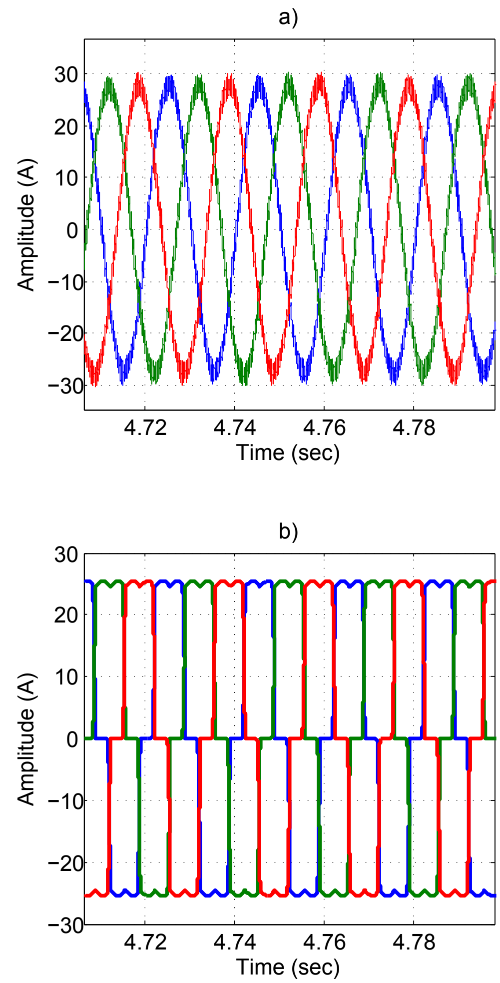


Fig. 6. Grid (a) and load (b) currents with ShAPF control.

VSC capacitor are taken into account to determine the main controller references.

In this case, the vectors for the harmonic frequencies are used, making plant inversion unnecessary. Note that the frequency response needed is the closed-loop of the plant together with the main controller (inner-current regulator). Only one PI controller has to be designed to be used for all the harmonics to be tackled. The cut-off frequency of the low-pass filter in charge of extracting the error signal for each harmonic can be tuned in order to change the selectiveness of the harmonic controllers; although, changes will also affect the closed-loop system speed.

In the simulation carried out, the harmonic controller has been set to tackle harmonics from the 5th to the 31st one and it was switched on at 0.5 seconds. Grid and load currents are shown in Figure 5 before the controller is switched on. Grid currents have a high-frequency noise produced by the converter. In this case, current harmonics are drawn by the rectifier-type load. Figure 6 shows the three-phase current results when the ShAPF using the EMRF controller is applied to compensate the current harmonics produced by the diode rectifier.

Fig. 7 shows the harmonic amplitudes in the grid currents before and after the controller is turned on. The selected harmonics are fully under control after 200 ms. Finally, the amplitudes of each harmonic of the load and grid currents with the ShAPF controller switched on are shown in Fig. 8. The resultant THDs of load and grid currents are 25.6% and 0.7%, respectively.

As mentioned before, the proposed control method can also adapt to grid frequency variations naturally and rapidly. This can be shown in Fig. 9 where the harmonic content of the grid currents is shown when, after 2 seconds of starting the experiment, the grid frequency ramps up from 50 Hz to 51 Hz in 1 second. Note that Fig. 9 is a zoom view of the grid current harmonic level with the EMRF controller turned on. According to Fig. 9, the harmonic level in the grid currents is still very low (under $2 \cdot 10e^{-3}$), with a THD is 25.5% and 0.6% for load and grid currents, respectively.

## VI. Summary and Conclusions

This paper proposes the use of an efficient multiple-reference-frame (EMRF) regulator for harmonic-current control in shunt active power filter applications, as an alternative to selective and repetitive controllers in a stationary

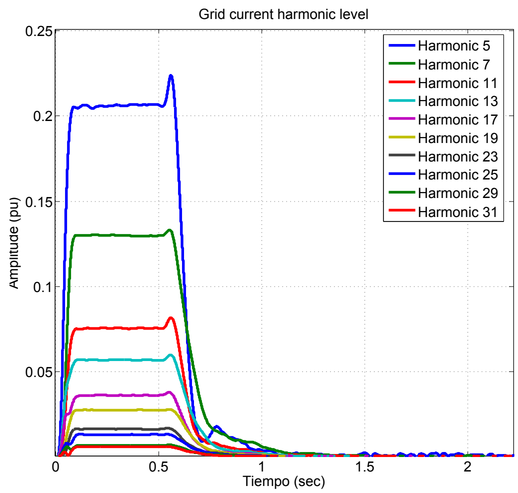


Fig. 7. Harmonic level in the grid currents before and after the EMRF is turned on

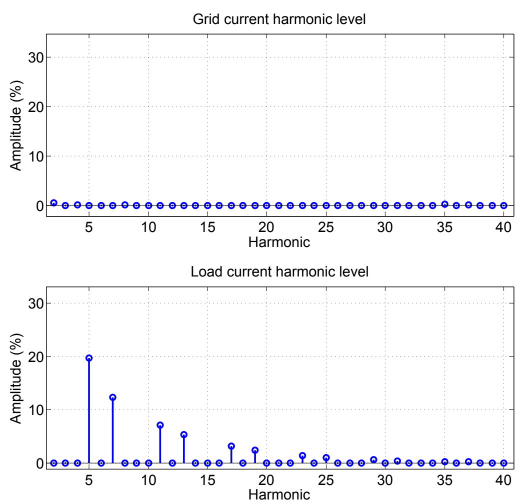


Fig. 8. Harmonic level in grid and load currents (50 Hz)

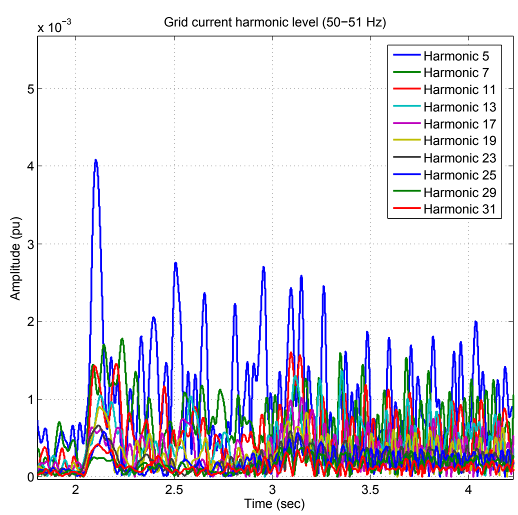


Fig. 9. Harmonic level in the grid currents when a grid-frequency change takes place

reference frame. It can be shown that PI controllers can be used to tackle each harmonic whilst the computation effort is maintained significantly lower than previously recognised. Frequency response of the plant is used instead of the transfer function for normalisation, making the implementation of the same PI regulator for each harmonic possible. Furthermore, it can also be shown that grid-frequency adaptation can be implemented naturally and harmonic control can respond very quickly to this variation. Simulation results of a ShAPF with SIMULINK-SIMPOWER show the effectiveness of the proposed control system.

## Acknowledgments

Thanks are due to the Spanish Government (ENE2011-28527-C04-01) for partially financing this work.

## References

[1] Badrul H. Chowdhury. Power quality. In *Potentials, IEEE*, pages 5–11, 2001.
[2] James K. Phipps, John P. Nelson, and Pankaj K. Sen. Power quality and harmonic distortion on distribution systems. In *Industry Applications, IEEE Transactions on*, pages 476–484, 1994.
[3] Yi Tang, Poh Chiang Loh, Peng Wang, Fook Hoong Choo, Feng Gao, and Frede Blaabjerg. Generalized design of high performance shunt active power filter with output LCL filter. In *IEEE Transactions on Industrial Electronics*, volume 59, pages 1443–1452, 2012.
[4] H. Rudnick, J. Dixon, and L. Moran. Delivering clean and pure power. In *Power and Energy Magazine, IEEE*, pages 32–40, 2003.
[5] V. Blasko, L. Arnedo, P. Kshirsagar, and S. Dwari. Control and elimination of sinusoidal harmonics in power electronics equipment: A system approach. In *Energy Conversion Congress and Exposition (ECCE), 2011 IEEE*, pages 2827–2837, 2011.
[6] D.N. Zmood and D.G. Holmes. Stationary frame current regulation of PWM inverters with zero steady-state error. In *IEEE Transactions on Power Electronics*, pages 814–822, 2003.
[7] X. Yuan, W. Merk, H. Stemmler, and J. Allmeling. Stationary frame generalized integrators for current control of active power filters with zero steady state error for current harmonics of concern under unbalanced and distorted operation conditions. In *IEEE Transactions on Industry Applications*, pages 523–532, 2002.
[8] M.J. Newman, D.N. Zmood, and D.G. Holmes. Stationary frame harmonic reference generation for active filter systems. In *IEEE Transactions on Industry Applications*, pages 1591–1599, 2002.
[9] J. Roldán-Pérez, A. García-Cerrada, J.L. Zamora-Macho, P. Roncero-Sánchez, and E. Acha. Adaptive repetitive controller for a three-phase dynamic voltage restorer. In *Power Engineering, Energy and Electrical Drives (POWERENG), 2011 International Conference on*, pages 1–6, 2011.
[10] S.J. Lee and S.-K. Sul. A harmonic reference frame based current controller for active filter. In *Proc. Applied Power Electronics Conference (APEC)*, pages 1073–1078, 2000.
[11] P. Mattavelli. A closed-loop selective harmonic compensation for active filters. In *IEEE Transactions on Industry Applications*, pages 81–89, 2001.
[12] D.N. Zmood, D.G. Holmes, and G.H. Bode. Frequency-domain analysis of three-phase linear current regulators. In *IEEE Transactions on Industry Applications*, pages 601–610, 2001.
[13] H. Lev-Ari and A.M. Stankovic. Customized dynamic phasors for power quality control in electric grids. In *Computational Advances in Multi-Sensor Adaptive Processing (CAMSAP), 2011 4th IEEE International Workshop on*, pages 129–132, 2011.
[14] J. Lee, D. H Kang, H. G Jeong, and K. B Lee. Active damping for large-scale wind power systems with an LCL-filter using an improved DFT. In *IECON 2011-37th Annual Conference on IEEE Industrial Electronics Society*, pages 1179–1184, 2011.
[15] P. Mattavelli. Synchronous-frame harmonic control for high-performance AC power supplies. In *IEEE Transactions on Industry Applications*, pages 864–872, 2001.
[16] M. Hazewinkel, editor. *Encyclopedia of Mathematics*. Springer, 2001.